



Pillared and open-framework uranyl diphosphonates

Pius O. Adelani^{a,b}, Thomas E. Albrecht-Schmitt^{a,b,*}

^a Department of Civil Engineering and Geological Sciences, 156 Fitzpatrick Hall, University of Notre Dame, Notre Dame, IN 46556, USA

^b Department of Chemistry and Biochemistry, 156 Fitzpatrick Hall, University of Notre Dame, Notre Dame, IN 46556, USA

ARTICLE INFO

Article history:

Received 18 February 2011

Received in revised form

17 June 2011

Accepted 26 June 2011

Available online 3 July 2011

Keywords:

Uranyl
Uranium
Phosphonate
Pillared structure

ABSTRACT

The hydrothermal reactions of uranium trioxide, uranyl acetate, or uranyl nitrate with 1,4-benzenediphosphonic acid in the presence of very small amount of HF at 200 °C results in the formation of three different uranyl diphosphonate compounds, $[\text{H}_3\text{O}]_2\{(\text{UO}_2)_6[\text{C}_6\text{H}_4(\text{PO}_3)(\text{PO}_2\text{OH})]_2[\text{C}_6\text{H}_4(\text{PO}_2\text{OH})_2]_2[\text{C}_6\text{H}_4(\text{PO}_3)_2](\text{H}_2\text{O})_2\}$ (**Ubbp-1**), $[\text{H}_3\text{O}]_4\{(\text{UO}_2)_4[\text{C}_6\text{H}_4(\text{PO}_3)_2\text{F}_4] \cdot \text{H}_2\text{O}\}$ (**Ubbp-2**), and $\{(\text{UO}_2)[\text{C}_6\text{H}_2\text{F}_2(\text{PO}_2\text{OH})_2(\text{H}_2\text{O})_2] \cdot \text{H}_2\text{O}\}$ (**Ubbp-3**). The crystal structures of these compounds were determined by single crystal X-ray diffraction experiments. **Ubbp-1** consists of UO_7 pentagonal bipyramids that are bridged by the phosphonate moieties to form a three-dimensional pillared structure. **Ubbp-2** is composed of UO_5F_2 pentagonal bipyramids that are bridged through the phosphonate oxygen atoms into one-dimensional chains that are cross-linked by the phenyl spacers into a pillared structure. The structure of **Ubbp-3** is a three-dimensional open-framework with large channels containing water molecules with internal dimensions of approximately $10.9 \times 10.9 \text{ \AA}$. **Ubbp-1** and **Ubbp-2** fluoresce at room temperature.

© 2011 Elsevier Inc. All rights reserved.

1. Introduction

The current interest in the structural chemistry of uranyl oxoanions is particularly evident with its recent expansion in literature; the number of different structure types of purely inorganic uranium(VI) compounds has increased from about 180 to over 368 between 1997 and 2005 [1]. One member of this large family that continues to yield unusual structural features and results are the phosphonates. The modification of the organic residues of phosphonates can lead to rich structural diversity and various coordination modes in actinide systems. Actinide phosphonates have relevance to nuclear waste management and separation processes [2]. Other potential applications have also been identified in ion-exchange [3], ionic conductivity [4], intercalation chemistry [5], photochemistry [6], non-linear optical materials [3g,7], and catalysis [5,8]. The structural chemistry of phosphonates is fascinating, displaying transformation from one-dimensional α - and β -uranyl phenylphosphonate to nanotubular γ -uranyl phenylphosphonate upon exposure to Na^+ or Ca^{2+} cations in aqueous solution [9]. Recently, we demonstrated that when Cs^+ cations are used to template the structure of uranyl phenyldiphosphonate a remarkable elliptical uranyl nanotubular structure results, $\text{Cs}_{3.62}\text{H}_{0.38}\{(\text{UO}_2)_4[\text{C}_6\text{H}_4(\text{PO}_2\text{OH})_2]_3[\text{C}_6\text{H}_4(\text{PO}_3)_2\text{F}_2]\}$ [10]. Immersion

of this compound in Ag^+ aqueous solution resulted in a partial exchange of the Cs^+ cations with Ag^+ .

There is a predisposition for actinide compounds to form low-dimensional structures because the terminal nature of the 'yl' oxo atoms of the actinyl unit favors the formation of layers of coordination polyhedra [11]. However, they have characteristic rich and diverse coordination environments favoring tetragonal, pentagonal, and hexagonal bipyramids in almost boundless combinations. Three-dimensional structures are rare. In order to circumvent this, additional building units have been utilized to make higher dimensional networks. We have made several two-dimensional and three-dimensional luminescent pillared uranyl diphosphonates with various protonated organic amines [12]. The inclusion of alkali and transition metals allow for the lower dimensional networks to be connected into three-dimensional frameworks. $\text{Cs}_3\{(\text{UO}_2)_4(\text{PO}_3\text{CH}_2\text{CO}_2)_2(\text{PO}_3\text{CH}_2\text{CO}_2\text{H}_{0.5})_2\} \cdot n\text{H}_2\text{O}$ is an example of where the uranyl polyhedra are connected to form a three-dimensional framework [13a], the addition of transition metals have been reported for the synthesis of three-dimensional frameworks of $[\text{H}_3\text{O}](\text{UO}_2)_2\text{Cu}_2(\text{PPA})_3(\text{H}_2\text{O})_2$ [13b] and $(\text{UO}_2)_2(\text{PPA})_2(\text{HPPA})\text{Zn}_2(\text{H}_2\text{O})_2 \cdot 3\text{H}_2\text{O}$ (PPA = phosphonoacetate) [13c]. Recent communication from our group demonstrates further how high symmetry cubic and rhombohedral space groups, porous heterobimetallic uranyl carboxyphosphonate can be constructed in the presence of disordered divalent transition metals [14]. As an extension of previous work we report the syntheses, structural characterization, and fluorescence properties of $[\text{H}_3\text{O}]_2\{(\text{UO}_2)_6[\text{C}_6\text{H}_4(\text{PO}_3)(\text{PO}_2\text{OH})]_2[\text{C}_6\text{H}_4(\text{PO}_2\text{OH})_2]_2[\text{C}_6\text{H}_4(\text{PO}_3)_2]\}(\text{H}_2\text{O})_2$, $[\text{H}_3\text{O}]_4\{(\text{UO}_2)_4[\text{C}_6\text{H}_4(\text{PO}_3)_2\text{F}_4] \cdot \text{H}_2\text{O}\}$ and $\{(\text{UO}_2)[\text{C}_6\text{H}_2\text{F}_2(\text{PO}_2\text{OH})_2(\text{H}_2\text{O})_2] \cdot \text{H}_2\text{O}\}$.

* Corresponding author at: Department of Civil Engineering and Geological Sciences, 156 Fitzpatrick Hall, University of Notre Dame, Notre Dame, IN 46556, USA.

E-mail address: talbrec1@nd.edu (T.E. Albrecht-Schmitt).

2. Experimental

2.1. Synthesis

$\text{UO}_2(\text{C}_2\text{H}_3\text{O}_2)_2 \cdot 2\text{H}_2\text{O}$ (98%, Alfa-Aesar), UO_3 (98% Strem), $\text{UO}_2(\text{NO}_3) \cdot 6\text{H}_2\text{O}$ (98%, International Bio-Analytical Industries), HF (48 wt%, Aldrich), 1,4-benzenebisphosphonic acid (95%, Epsilon Chimie) were used as received. Reactions were run in PTFE-lined Parr 4749 autoclaves with a 23 mL internal volume. Distilled and Millipore filtered water with resistance of 18.2 M Ω cm was used in all reactions. **Caution!** While all the uranium compounds used in these studies contained depleted uranium salts, standard precautions were performed for handling radioactive materials, and all studies were conducted in a laboratory dedicated to studies on actinide elements.

2.2. $[\text{H}_3\text{O}]_2\{(\text{UO}_2)_6[\text{C}_6\text{H}_4(\text{PO}_3)(\text{PO}_2\text{OH})]_2[\text{C}_6\text{H}_4(\text{PO}_2\text{OH})_2]_2[\text{C}_6\text{H}_4(\text{PO}_3)_2]\}(\text{H}_2\text{O})_2$ (*Ubbp-1*)

UO_3 (57.3 mg, 0.2 mmol), 1,4-benzenebisphosphonic acid (47.6 mg, 0.2 mmol), 1.0 mL of water, and a very small quantities of HF were loaded into a 23 mL autoclave. The autoclave was sealed and heated to 200 °C in a box furnace for 3 days and was then cooled at an average rate of 5 °C/h to 25 °C. The resulting yellow product was washed with distilled water and methanol and allowed to air dry at room temperature. Yellow tablets of **Ubbp-1** as a pure phase suitable for X-ray diffraction studies were formed.

2.3. $[\text{H}_3\text{O}]_4\{(\text{UO}_2)_4[\text{C}_6\text{H}_4(\text{PO}_3)_2]_2\text{F}_4\} \cdot \text{H}_2\text{O}$ (*Ubbp-2*)

$\text{UO}_2(\text{C}_2\text{H}_3\text{O}_2)_2 \cdot 2\text{H}_2\text{O}$ (84.8 mg, 0.2 mmol), 1,4-benzenebisphosphonic acid (47.7 mg, 0.2 mmol), 0.5 mL of water, and a very small quantities of HF were loaded into a 23 mL autoclave. The autoclave was sealed and heated to 200 °C in a box furnace for 3 days. The autoclave was then cooled at an average rate of 5 °C/h to 25 °C. The resulting yellow product was washed with distilled water and methanol and allowed to air dry at room temperature. Yellow tablets of **Ubbp-2** with some minor impurities were formed.

2.4. $\{(\text{UO}_2)[\text{C}_6\text{H}_2\text{F}_2(\text{PO}_2\text{OH})_2(\text{H}_2\text{O})]_2\} \cdot \text{H}_2\text{O}$ (*Ubbp-3*)

$\text{UO}_2(\text{NO}_3) \cdot 6\text{H}_2\text{O}$ (100.5 mg, 0.2 mmol) along with 1,4-benzenebisphosphonic acid (47.6 mg, 0.2 mmol), 0.5 mL of water, and a very small quantities of HF were loaded into a 23 mL autoclave. After heating for 3 days at 200 °C, the autoclave was then cooled at an average rate of 5 °C/h to 25 °C. The resulting yellow product was washed with distilled water and methanol and allowed to air dry at room temperature. Yellow needles of **Ubbp-3** along with unidentifiable powder were formed. Attempts to increase the yield and purity of **Ubbp-3** by adjusting the reaction temperature, heating time and ratios of reactants did not result in producing a pure product.

2.5. Crystallographic studies

Single crystals of **Ubbp-1**, **2**, and **3** were mounted on glass fibers and optically aligned on a Bruker APEXII CCD X-ray diffractometer using a digital camera. Initial intensity measurements were performed using a λ μS X-ray source, a 30 W micro-focused sealed tube (MoK α , $\lambda = 0.71073$ Å) with a monocapillary collimator. Standard APEXII software was used for determination of the unit cells and data collection control. The intensities of reflections of a sphere were collected by a combination of four sets of exposures (frames). Each set had a different φ angle for the

crystal and each exposure covered a range of 0.5° in ω . A total of 1464 frames were collected with an exposure time per frame of 10–30 s, depending on the crystal. SAINT software was used for data integration including Lorentz and polarization corrections. Semi-empirical absorption corrections were applied using the program SADABS [15]. The program suite SHELXTL was used for space group determination (XPREP), direct methods structure solution (XS), and least-squares refinement (XL) [16]. The position of H atoms around the H_2O or OH were located and refined freely while those around the benzene ring were added using the xprep command 'hadd'. The final refinements included anisotropic displacement parameters for all atoms except H atoms. Selected crystallographic information is listed in Table 1. Atomic coordinates, bond distances, and additional structural information are provided in the Supplementary information (CIF's).

2.6. Fluorescence spectroscopy

Fluorescence data for **Ubbp-1** and **Ubbp-2** were acquired from single crystals using a Craic Technologies UV-vis-NIR microspectrophotometer with a fluorescence attachment. Excitation was achieved using 365 nm light from a mercury lamp for the fluorescence spectroscopy.

3. Results and discussion

3.1. Synthesis

All three uranyl phosphonates, **Ubbp-1**, **Ubbp-2**, and **Ubbp-3**, were prepared using three different uranium salts under mild hydrothermal conditions. The stoichiometric ratio of 1:1 (U:P) were used in all the syntheses. The addition of HF to the reactions is essential, and it serves as a mineralizing agent in the syntheses, as ligand in the formation of **Ubbp-2**, as well as for the purpose of fluorination of the phenyl ring in **Ubbp-3**.

3.2. General structural characteristics

$[\text{H}_3\text{O}]_2\{(\text{UO}_2)_6[\text{C}_6\text{H}_4(\text{PO}_3)(\text{PO}_2\text{OH})]_2[\text{C}_6\text{H}_4(\text{PO}_2\text{OH})_2]_2[\text{C}_6\text{H}_4(\text{PO}_3)_2]\}(\text{H}_2\text{O})_2$ (**Ubbp-1**) crystallizes in the centrosymmetric, triclinic space group $P\bar{1}$, and the coordination environment uranium atoms are found

Table 1

Crystallographic data for $[\text{H}_3\text{O}]_2\{(\text{UO}_2)_6[\text{C}_6\text{H}_4(\text{PO}_3)(\text{PO}_2\text{OH})]_2[\text{C}_6\text{H}_4(\text{PO}_2\text{OH})_2]_2[\text{C}_6\text{H}_4(\text{PO}_3)_2]\}(\text{H}_2\text{O})_2$ (**Ubbp-1**), $[\text{H}_3\text{O}]_4\{(\text{UO}_2)_4[\text{C}_6\text{H}_4(\text{PO}_3)_2]_2\text{F}_4\} \cdot \text{H}_2\text{O}$ (**Ubbp-2**), and $\{(\text{UO}_2)[\text{C}_6\text{H}_2\text{F}_2(\text{PO}_2\text{OH})_2(\text{H}_2\text{O})]_2\} \cdot \text{H}_2\text{O}$ (**Ubbp-3**).

Compound	Ubbp-1	Ubbp-2	Ubbp-3
Formula mass	1428.17	1704.18	1128.09
Color and habit	Yellow, tablet	Yellow, tablet	Yellow, needle
Space group	$P\bar{1}$	<i>Cmcm</i>	$P4_2/nmc$
<i>a</i> (Å)	9.9612(3)	17.9546(7)	20.3539(16)
<i>b</i> (Å)	10.9029(4)	7.0283(3)	20.3539(16)
<i>c</i> (Å)	14.5948(5)	25.0796(9)	7.8010(6)
α (deg.)	90.0421(3)	90	90
β (deg.)	109.3749(3)	90	90
γ (deg.)	92.6223(3)	90	90
<i>V</i> (Å ³)	1493.54(9)	3164.8(2)	3231.8(4)
<i>Z</i>	2	4	4
<i>T</i> (K)	100	100	100
λ (Å)	0.71073	0.71073	0.71073
ρ_{calcd} (g cm ⁻³)	3.174	3.577	2.319
μ (Mo K α) (mm ⁻¹)	16.588	20.728	10.298
<i>R</i> (<i>F</i>) for $F_0^2 > 2\sigma(F_0^2)^a$	0.0219	0.0208	0.0391
$R_w(F_0^2)^b$	0.049	0.049	0.114

^a $R(F) = \sum |F_0| - |F_c| / \sum |F_0|$.

^b $R(F_0^2) = [\sum w(F_0^2 - F_c^2)^2 / \sum w(F_0^2)]^{1/2}$.

as UO_7 pentagonal bipyramids, this represent most common coordination environment in uranium [11]. The UO_7 units contain a layered central uranyl cation, UO_2^{2+} , that are bridged by the phosphonate moieties to form three-dimensional pillared structure (Fig. 1). Two of the uranyl cations share an edge via bridging oxygen atoms as depicted in Fig. 2. A view along the $[bc]$ plane reveals the uranyl dimers that are connected into sheets of uranyl polyhedral

through the oxygen and μ_2 -O atoms of the phosphonate ligands. This structure contains hydronium ions, so that charge balance is maintained (Tables 2–4).

The structure consists of three crystallographically unique uranyl centers, U(1), U(2), and U(3). Uranium atoms typically coordinate with two nearly linear oxo atoms, UO_2^{2+} cations, for the three uranium centers, the $\text{O}=\text{U}=\text{O}$ bond angles are $179.66(16)^\circ$, $178.71(16)^\circ$ and $179.57(15)^\circ$ and normal average

Table 2

Selected bond distances (Å) and angles (deg.) for $[\text{H}_3\text{O}]_2\{(\text{UO}_2)_6[\text{C}_6\text{H}_4(\text{PO}_3)_2(\text{PO}_2\text{OH})_2]_2[\text{C}_6\text{H}_4(\text{PO}_3)_2]\}(\text{H}_2\text{O})_2$ (**Ubbp-1**).

Distances (Å)			
U(1)–O(1)	1.764(3)	P(1)–O(10)	1.501(4)
U(1)–O(2)	1.767(3)	P(1)–O(8)	1.522(4)
U(1)–O(8)	2.297(3)	P(1)–O(9)	1.555(4)
U(1)–O(20)	2.372(4)	P(1)–C(10)	1.783(5)
U(1)–O(11)	2.414(3)	P(2)–O(13)	1.512(3)
U(1)–O(17)	2.425(3)	P(2)–O(11)	1.529(3)
U(1)–O(12)	2.546(3)	P(2)–O(12)	1.554(3)
U(2)–O(3)	1.763(3)	P(2)–C(11)	1.786(5)
U(2)–O(4)	1.777(3)	P(3)–O(15)	1.493(3)
U(2)–O(15)	2.330(3)	P(3)–O(16)	1.523(3)
U(2)–O(10)	2.339(3)	P(3)–O(14)	1.568(3)
U(2)–O(19)	2.355(3)	P(3)–C(9)	1.793(5)
U(2)–O(13)	2.408(3)	P(4)–O(19)	1.493(3)
U(2)–O(7)	2.487(3)	P(4)–O(17)	1.547(3)
U(3)–O(6)	1.764(3)	P(4)–O(18)	1.564(3)
U(3)–O(5)	1.785(3)	P(4)–C(5)	1.787(5)
U(3)–O(16)	2.284(3)	P(5)–O(20)	1.492(4)
U(3)–O(12)	2.334(3)	P(5)–O(22)	1.534(5)
U(3)–O(18)	2.370(3)	P(5)–O(21)	1.584(4)
U(3)–O(17)	2.496(3)	P(5)–C(6)	1.793(5)
U(3)–O(11)	2.512(3)		
Angles (deg.)			
O(2)–U(1)–O(1)	179.66(16)	O(3)–U(2)–O(4)	178.71(16)
O(5)–U(3)–O(6)	179.57(15)		

Table 3

Selected bond distances (Å) and angles (deg.) for $[\text{H}_3\text{O}]_4\{(\text{UO}_2)_4[\text{C}_6\text{H}_4(\text{PO}_3)_2]_2\text{F}_4\} \cdot \text{H}_2\text{O}$ (**Ubbp-2**).

Distances (Å)			
U(1)–O(2)	1.776(4)	U(1)–F(2)	2.378(2)
U(1)–O(1)	1.790(4)	P(1)–O(5)	1.521(3)
U(1)–O(4i)	2.280(3)	P(1)–O(4)	1.525(3)
U(1)–O(5ii)	2.314(3)	P(1)–O(3)	1.532(3)
U(1)–O(3)	2.334(3)	P(1)–C(1)	1.802(4)
U(1)–F(1)	2.366(2)		
Angles(deg.)			
O(2)–U(1)–O(1)		176.99(16)	

Table 4

Selected bond distances (Å) and angles (deg.) for $\{(\text{UO}_2)[\text{C}_6\text{H}_2\text{F}_2(\text{PO}_2\text{OH})_2(\text{H}_2\text{O})]\}_2 \cdot \text{H}_2\text{O}$ (**Ubbp-3**).

Distances (Å)			
U(1)–O(1)	1.787(8)	P(1)–O(4)	1.502(6)
U(1)–O(2)	1.789(8)	P(1)–O(5)	1.489(6)
U(1)–O(4)	2.299(5)	P(1)–O(6)	1.565(7)
U(1)–O(4')	2.299(6)	P(1)–C(1)	1.799(8)
U(1)–O(5)	2.346(6)	C(2)–F(1)	1.714(10)
U(1)–O(5')	2.346(6)		
U(1)–O(3)	2.561(9)		
Angles (deg.)			
O(2)–U(1)–O(1)	179.0(4)		

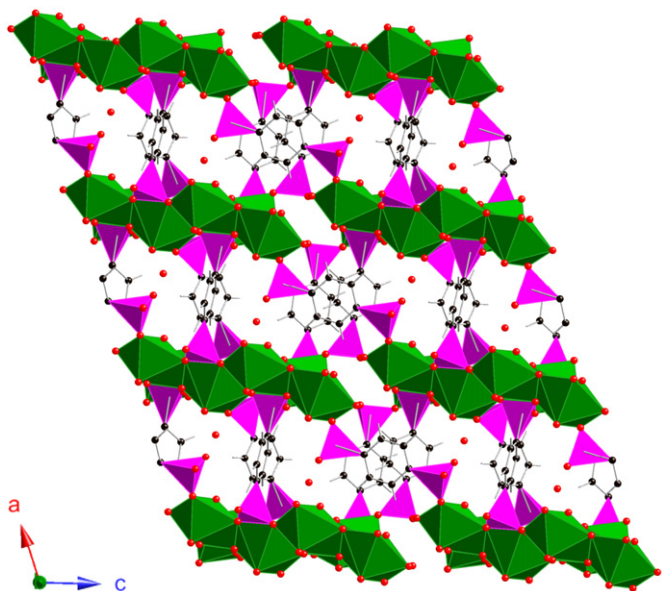


Fig. 1. Polyhedral representation of the three-dimensional pillared structure of **Ubbp-1** viewed along the b axis. The structure is constructed from UO_7 units, pentagonal bipyramids=green, oxygen=red, phosphorus=magenta, carbon=black and hydrogen=white. (For interpretation of the references to color in this figure legend, the reader is referred to the web version of this article.)

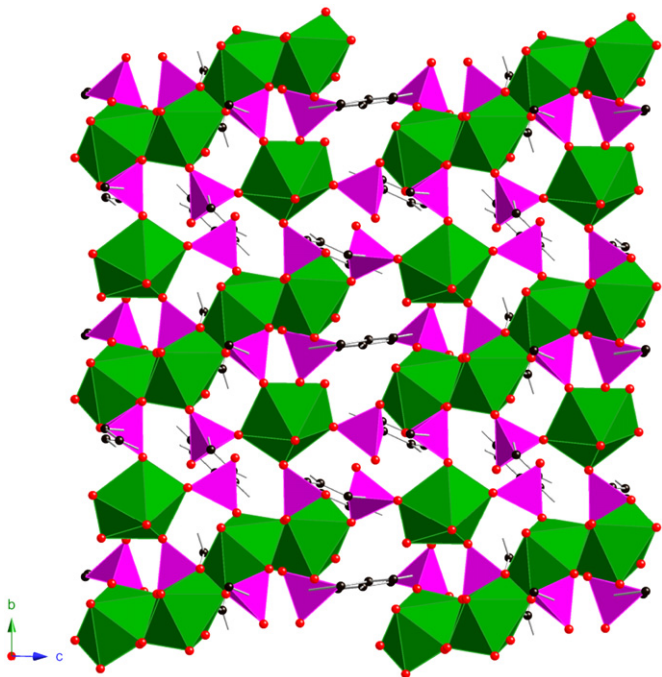


Fig. 2. Polyhedral representation of the **Ubbp-1** viewed along the $[bc]$ plane. The structure is constructed from UO_7 units, pentagonal bipyramids=green, oxygen=red, phosphorus=magenta, carbon=black and hydrogen=white. (For interpretation of the references to color in this figure legend, the reader is referred to the web version of this article.)

U=O bond distances of 1.766(3), 1.770(3) and 1.775(3) Å, respectively. The equatorial U–O bond distances vary considerably. U(1) coordinates to three short U–O bonds from phosphonate ligands that range from 2.297(3) to 2.414 (3) Å. There are two bridging μ_2 -O atoms with longer U–O bond distances of 2.425(3) and 2.546(3) Å. In addition, one of the four different phosphonate ligands coordinates to uranium center in bidentate fashion. For U(2), there are four short equatorial U–O bonds from phosphonate O-atoms that range from 2.330(3) to 2.408(3) Å. The longest U–O bond distance of 2.487(3) Å is also terminal, we therefore assigned it as a coordinating water molecule. U(3) is similar to the U(1) center, it is coordinated by one short U(3)–O(16) bond of 2.284(3) Å from phosphonate ligand. The remaining four are from bridging μ_2 -O atoms of the phosphonate ligands and range from 2.334(3) to 2.512(3) Å. A total of three phosphonate ligands are involved in the coordination to uranium centers and one of them is bidentate pattern. These distances were used to calculate bond-valence sums of 6.00, 6.09 and 6.00 for U(1), U(2), and U(3), respectively, they all agree well with the formal oxidation state of +6 [11]. The P–O bond distances range from 1.492(4) to 1.584(4) Å. The P–O bonds can be distinguished from the P–OH bonds base on the bond lengths and whether or not they are coordinating to uranium center. We therefore propose that the long P–O bond distances that are terminal belong to the protonated phosphonate-oxygen groups.

3.3. Structure of $[H_3O]_4\{(UO_2)_4[C_6H_4(PO_3)_2]_2F_4\} \cdot H_2O$ (*Ubbp-2*)

The result from single crystal X-ray diffraction experiments revealed that **Ubbp-2** crystallizes in the orthorhombic space group *Cmcm*, has one crystallographically unique uranium center in a UO_5F_2 pentagonal bipyramid, and that the structure is layered. It consists of uranyl cations, UO_2^{2+} , that are bridged through the phosphonate moieties into a one-dimensional chain. The chains are cross-linked by the rigid phenyl spacers into a pillared structure as shown in Fig. 3. A view along the *c*-axis

(Fig. 4) reveals pentagonal bipyramids with edge-sharing fluoride atoms to form uranyl dimers. These dimers are joined into sheets of uranyl polyhedra through the PO_3 moieties. The presence of H_3O^+ ions are essential to compensate for the charges from the anionic layers, $\{(UO_2)_4[C_6H_4(PO_3)_2]_2F_4\}^{4-}$.

The uranium(VI) site is bound to two axial oxygen atoms with U=O bond distances of 1.790 (4) and 1.776(4) Å and an O=U=O bond angle of 176.99(16)°. The U–O bonds along the

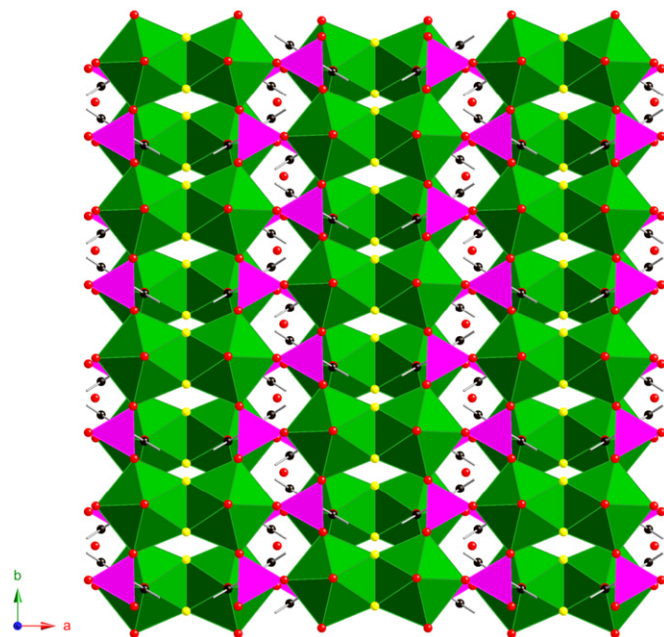


Fig. 4. Illustration along the *c*-axis of **Ubbp-2**. The structure is constructed from UO_5F_2 units, pentagonal bipyramids=green, fluoride=yellow, oxygen=red, phosphorus=magenta, carbon=black, hydrogen=white. (For interpretation of the references to color in this figure legend, the reader is referred to the web version of this article.)

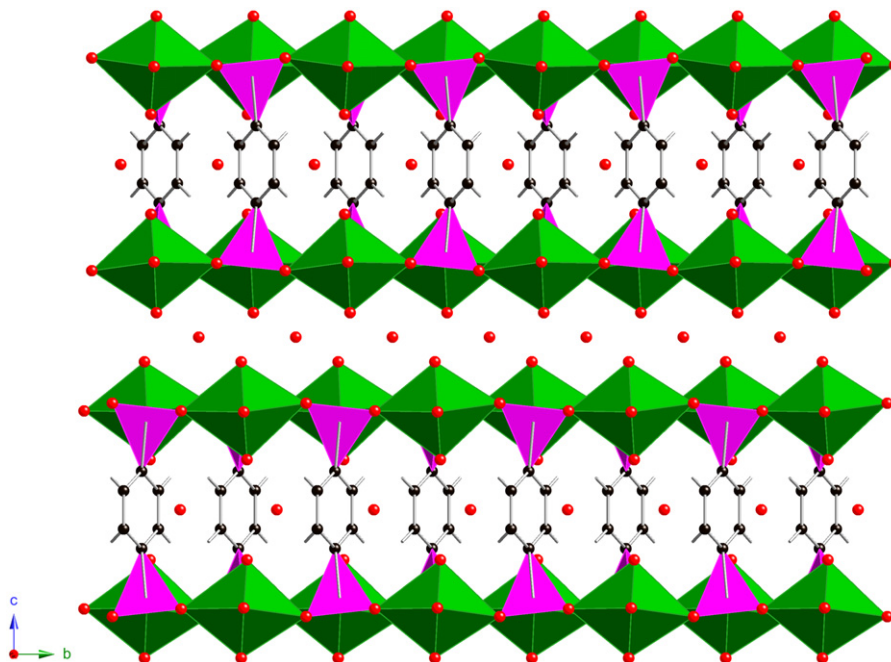


Fig. 3. A depiction of the layers in **Ubbp-2** viewed along the *a* axis. The structure is constructed from UO_5F_2 units, pentagonal bipyramids=green, fluoride=yellow, oxygen=red, phosphorus=magenta, carbon=black and hydrogen=white.(For interpretation of the references to color in this figure legend, the reader is referred to the web version of this article.)

equatorial axis are shorter than the U–F bonds, showing bond distances of 2.334(3), 2.280(3) and 2.314(3) Å for O(3), O(4) and O(5), respectively, while the F(1) and F(2) are at distances 2.366(2) and 2.378(2) Å from uranium center. The assignments of either F or O atoms were made based on the improvements in the refinements when the correct element was selected. Typically when the element was incorrectly identified, it became nonpositive definite when refined anisotropically. Energy dispersive spectrometer (EDS) analysis also confirmed the presence of F atoms. The bond-valence sum calculation of 5.85 from these bonds is consistent with U(VI) [11]. The phosphonate oxygen atoms are completely deprotonated with average P–O bond distance of 1.526(3) Å.

3.4. $\{(UO_2)[C_6H_2F_2(PO_2OH)_2(H_2O)]_2 \cdot H_2O\}$ (*Ubbp-3*)

The structure of **Ubbp-3** is remarkable and different from the other two previously discussed structures. **Ubbp-3** consists of chains of UO_7 pentagonal bipyramids that are connected through the phosphonate moiety into a three-dimensional open-framework structure. It adopts a tetragonal space group $P4_2/nmc$, this is an uncommon space group among the uranyl phenylphosphonates. There are large channels that run parallel to *c*-axis as shown in Fig. 5. These large channels contain water molecules with internal dimensions of approximately 10.9×10.9 Å. The pores consist of four uranyl units and four phenyldiphosphonates that are alternatively connected. It is important to point out that two of the carbons of the phenyl rings are fluorinated with the fluorine atoms pointing into the channels, which confers on it a unique structure. There are also small channels that are connected through the uranyl units with pores size of approximately 2.9×2.9 Å.

This structure incorporates UO_7 pentagonal bipyramids, the most common form among the uranyl compounds [1,11]. There is a crystallographically unique uranyl center, that is nearly linear with $[O=U=O]^{2+}$ bond angle of $179.0(4)^\circ$ and U=O bond distances of 1.787(8) and 1.789(8) Å. Four oxygen atoms from the

phosphonate are arranged perpendicular to the uranyl axis, and the U–O bond distances range from 2.299(5) to 2.346(6) Å. The fifth U–O bond of 2.561(9) Å corresponds to terminal oxygen atom, and therefore is a coordinated water molecule. Using these bond distances, we arrived at bond-valence sum of 6.07, which is consistent with the oxidation state of uranium(VI) [11]. The P(1)–O(6) bond distance of 1.565(7) Å is the longest P–O bond distance and correspond to the terminal oxygen atom, this is the site of protonation. We also observed a C–F bond distance of 1.714(10) Å (Fig. 6).

3.5. Fluorescence spectroscopy

The emission of green light centered near 520 nm by compounds containing uranyl cations has been known for centuries [17]. When compounds containing UO_2^{2+} moiety are excited with UV light, they exhibit a series of strongly vibronically-coupled charge-transfer features. It typically consists of a five-peak spectrum, far more lines can be observed at low temperature. Nevertheless, not all uranyl compounds fluoresce and the mechanisms of the emission from uranyl containing compounds are complex. Grohol and Clearfield reported a considerable variance in the luminescence properties of two closely related uranyl phenylphosphonate compounds, $[UO_2(HO_3PC_6H_5)_2(H_2O)]_2 \cdot 8H_2O$ and $UO_2(HO_3PC_6H_5)_2(H_2O) \cdot 2H_2O$, whose structural differences are based on the conformational differences of the phosphonate anions [9c]. As shown in Fig. 7, only **Ubbp-1** and **Ubbp-2** compounds are luminescent, and show the classical fluorescence spectra of uranyl compounds with five clearly resolved vibronic transitions. **Ubbp-3** did not fluoresce like other compounds. Joshi et al. [18a] demonstrated in their studies on lanthanide diketonates that fluorine substituent increases the fluorescence intensity because it decreases vibrational energy. This observation has been supported further by results on fluorinated 4-pyridylethynyl complex with rigid rods and Zn metal ion [18b]. Although, there have also been certain anomalies reported in

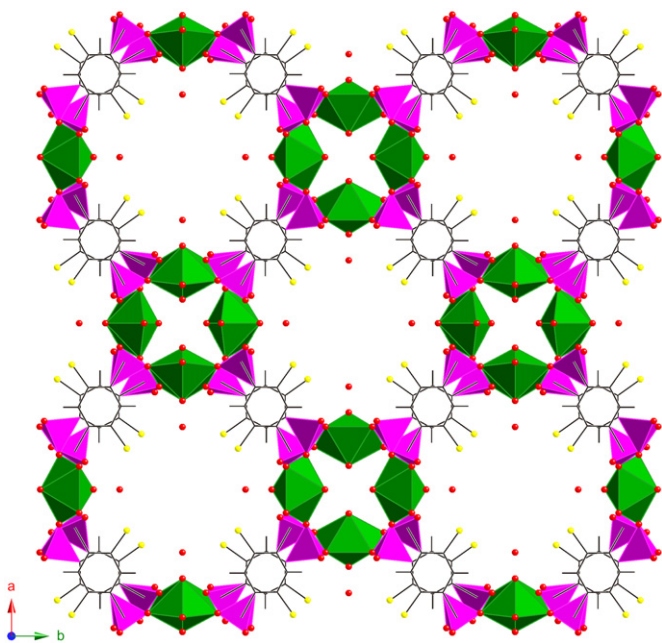


Fig. 5. Illustration of the three-dimensional open-framework structure of **Ubbp-3** viewed along the *c*-axis. The structure is constructed from UO_7 units, pentagonal bipyramids=green, oxygen=red, phosphorus=magenta, carbon=black and hydrogen=white. (For interpretation of the references to color in this figure legend, the reader is referred to the web version of this article.)

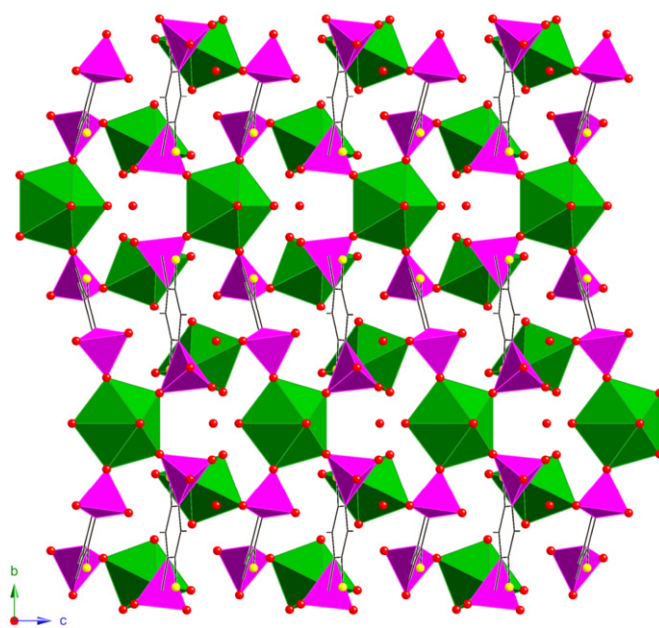


Fig. 6. View of the uranyl chains connected by the phosphonate ligand in **Ubbp-3**. The structure is constructed from UO_7 units, pentagonal bipyramids=green, oxygen=red, phosphorus=magenta, carbon=black and hydrogen=white. (For interpretation of the references to color in this figure legend, the reader is referred to the web version of this article.)

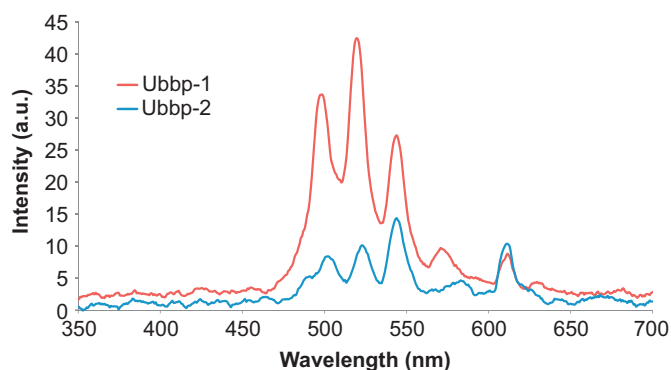


Fig. 7. Fluorescence spectrum of **Ubbp-1** and **Ubbp-2** showing five clearly resolved vibronically-coupled charge-transfer transitions.

fluorinated benzenes [19]. The fluorinated phenyl ring, the bonding and topology of **Ubbp-3** structure might be playing vital roles here.

4. Conclusions

The purpose of this work was to critically examine how the uranyl salt anions influence the structural chemistry of uranyl diphosphonate. There is a clear structural variation as we change the uranyl salts. One possibility is to assume that the acetate and nitrate counter ions of uranyl salts are acting as structure directing agents in these syntheses. Both are inner-sphere ligands for UO_2^{2+} . Moreover, a change of about 2 in pH units from replacement of uranyl nitrate with acetate is likely to influence these structural changes [12]. The use of rigid phenyl spacer allows for the synthesis of a pillar compounds [10,12]. The position of the phosphonate functional group via para-substituent on benzene ring is an important driving force for the observation of three-dimensional networks in these structures, a variation in position of the substituent results in low-dimensional networks observed when the substituent is in ortho-position [20]. The mineralizing agent, HF, is also often incorporated into products where it forms metal fluoride bonds, but this is the first time we observed the fluorination of the phenyl ring in our system under hydrothermal condition. Fluorinated aryl groups are versatile intermediates for the syntheses of various complexes and functionalized derivatives. This conversion can be carried out using HF in the presence of base as reported in the several literatures [21]. The large voids in this structure are suggestive of some unique characteristic properties for potential applications in sorption, separation of gases and in catalytic processes, the difficulty of obtaining a pure phase of **Ubbp-3** did not allow us to examine these properties further [14]. However, the central issue that will be addressed in future studies is to develop alternative route for the fluorination of the benzene ring and subsequent coordination to uranyl cation to yield the pure phase uranyl phosphonate framework.

Supporting information

Further details of the crystal structure investigation may be obtained from the Cambridge Crystallographic Data Center on quoting numbers CCDC 809134, 809135, and 809136.

Acknowledgments

We are grateful for support provided by the Chemical Sciences, Geosciences, and Biosciences Division, Office of Basic Energy Sciences,

Office of Science, Heavy Elements Program, U.S. Department of Energy, under Grant DE-FG02-01ER16026 and DE-SC0002215.

References

- [1] (a) P.C. Burns, M.L. Miller, R.C. Ewing, *Can. Mineral.* 34 (1996) 845; (b) P.C. Burns, in: P.C. Burns, R. Finch (Eds.), *In Uranium: Mineralogy, Geochemistry and the Environment*, Mineralogical Society of America, Washington, DC, 1999 Ch. 1; (c) P.C. Burns, *Mater. Res., Soc. Symp. Proc.* 802 (2004) 89; (d) P.C. Burns, *Can. Mineral.* 43 (2005) 1839–1894.
- [2] (a) K.L. Nash, *J. Alloys Compd.* 213–214 (1994) 300; (b) K.L. Nash, *J. Alloys Compd.* 249 (1997) 33; (c) M.P. Jensen, J.V. Beitz, R.D. Rogers, K.L. Nash, *J. Chem. Soc. Dalton Trans.* 18 (2000) 3058.
- [3] (a) G.H. Dieckmann, A.B. Ellis, *Solid State Ionics* 32/33 (1989) 50; (b) R. Vochten, *Am. Mineral.* 75 (1990) 221; (c) J. Benavente, J.R. Ramos Barrado, A. Cabeza, S. Bruque, M. Martinez, *Colloids Surf. A* 97 (1995) 13; (d) T.Y. Shvareva, P.M. Almond, T.E. Albrecht-Schmitt, *J. Solid State Chem.* 178 (2005) 499; (e) T.Y. Shvareva, T.A. Sullens, T.C. Shehee, T.E. Albrecht-Schmitt, *Inorg. Chem.* 44 (2005) 300; (f) T.Y. Shvareva, S. Skanthkumar, L. Soderholm, A. Clearfield, T.E. Albrecht-Schmitt, *Chem. Mater.* 19 (2007) 132; (g) K.M. Ok, J. Baek, P.S. Halasyamani, D. O'Hare, *Inorg. Chem.* 45 (2006) 10207.
- [4] (a) D. Grohol, E.L. Blinn, *Inorg. Chem.* 36 (1997) 3422; (b) C.H. Johnson, M.G. Shilton, A.T. Howe, *J. Solid State Chem.* 37 (1981) 37; (c) L. Moreno-Real, R. Pozas-Tormo, M. Martinez-Lara, S. Bruque-Gamez, *Mater. Res. Bull.* 22 (1987) 29; (d) R. Pozas-Tormo, L. Moreno-Real, M. Martinez-Lara, E. Rodriguez-Castellon, *Can. J. Chem.* 64 (1986) 35; (e) S. Obbade, C. Dion, M. Saadi, F. Abraham, *J. Solid State Chem.* 177 (2004) 1567; (f) S. Obbade, L. Duviour, C. Dion, F. Abraham, *J. Solid State Chem.* 180 (2007) 866.
- [5] A. Clearfield, *Prog. Inorg. Chem.* 47 (1998) 371.
- [6] (a) P.M. Almond, C.E. Talley, A.C. Bean, S.M. Peper, T.E. Albrecht-Schmitt, *J. Solid State Chem.* 154 (2000) 635; (b) M. Frisch, C.L. Cahill, *Dalton Trans.* 39 (2006) 4679; (c) C.L. Cahill, D.T. de Lill, M. Frisch, *Cryst. Eng. Commun.* 9 (2007) 15.
- [7] R.E. Sykora, T.E. Albrecht-Schmitt, *Inorg. Chem.* 47 (2003) 2179.
- [8] (a) G. Cao, H.-G. Hong, T.E. Mallouk, *Acc. Chem. Res.* 25 (1992) 420; (b) A. Clearfield, *Curr. Opin. Solid State Mater. Sci.* 6 (2003) 495; (c) J.-G. Mao, *Coord. Chem. Rev.* 251 (2007) 1493.
- [9] (a) D. Grohol, A. Clearfield, *J. Am. Chem. Soc.* 119 (1997) 9301; (b) D. Grohol, A. Clearfield, *J. Am. Chem. Soc.* 119 (1997) 4662; (c) D. Grohol, M.A. Subramanian, D.M. Poojary, A. Clearfield, *Inorg. Chem.* 35 (1996) 5264; (d) M.A.G. Aranda, A. Cabeza, S. Bruque, D.M. Poojary, A. Clearfield, *Inorg. Chem.* 37 (1998) 1827; (e) D.M. Poojary, A. Cabeza, M.A.G. Aranda, S. Bruque, A. Clearfield, *Inorg. Chem.* 35 (1996) 1468; (f) D.M. Poojary, D. Grohol, A. Clearfield, *Angew. Chem. Int. Ed. Engl.* 34 (1995) 1508.
- [10] P.O. Adelani, T.E. Albrecht-Schmitt, *Angew. Chem. Int. Ed. Engl.* 49 (2010) 8909.
- [11] (a) P.C. Burns, R.C. Ewing, F.C. Hawthorne, *Can. Mineral.* 35 (1997) 1551; (b) N.E. Brese, M. O'Keefe, *Acta Crystallogr.* B47 (1991) 192.
- [12] P.O. Adelani, T.E. Albrecht-Schmitt, *Inorg. Chem.* 48 (2009) 2732.
- [13] (a) A.N. Alsobrook, T.E. Albrecht-Schmitt, *Inorg. Chem.* 48 (2009) 11079; (b) A.N. Alsobrook, W. Zhan, T.E. Albrecht-Schmitt, *Inorg. Chem.* 47 (2008) 5177; (c) K.E. Knope, C.L. Cahill, *Eur. J. Inorg. Chem.* 8 (2010) 1177.
- [14] A.N. Alsobrook, B.G. Hauser, J.T. Hupp, E.V. Alekseev, W. Depmeier, T.E. Albrecht-Schmitt, *Chem. Commun.* 46 (2010) 9167.
- [15] G.M. Sheldrick, SADABS, Program for absorption correction using SMART CCD based on the method of Blessing: Blessing R. H., *Acta Crystallogr.* A51 (1995) 33.
- [16] G.M. Sheldrick, P.C. SHELXTL, Version 6.12, An Integrated System for Solving, Refining, and Displaying Crystal Structures from Diffraction Data, Siemens Analytical X-Ray Instruments, Inc., Madison, WI, 2001.
- [17] (a) G. Liu, J.V. Beitz, in: L.R. Morss, N.M. Edelstein, J. Fuger (Eds.), *The Chemistry of the Actinide and Transactinides Elements*, Springer, Heidelberg, 2006, p. 2088; (b) R.G. Denning, J.O.W. Norris, I.G. Short, T.R. Snellgrove, D.R. Woodward, in: N.M. Edelstein (Ed.), *Lanthanide and Actinide Chemistry and Spectroscopy* (ACS Symposium Series No. 131), Am. Chem. Soc., Washington, DC, 1980 Chap. 15.
- [18] (a) K.C. Joshi, V.N. Pathak, S.J. Bhargava, *Fluorine Chem* 9 (1977) 387; (b) T.M. Fasina, J.C. Collings, D.P. Lydon, D. Albesa-Jove, A.S. Batsanov, J.A.K. Howard, P. Nguyen, M. Bruce, A.J. Scott, W. Clegg, S.W. Watt, C. Viney, T.B.J. Marder, *Mater. Chem.* 14 (2004) 2395.
- [19] M.Z. Zgierski, T. Fujiwara, E.C. Lim, *J. Chem. Phys.* 122 (2005) 144312.
- [20] J. Diwu, S. Wang, Z. Liao, P.C. Burns, T.E. Albrecht-Schmitt, *Inorg. Chem.* 49 (2010) 10074.
- [21] V.D. Romanenko, V.P. Kukhar, *Chem. Rev.* 106 (2006) 3868.